NANOTHERMITE-BASED MICROSYSTEM FOR DRUG DELIVERY AND CELL TRANSFECTION

S. Apperson, R. Thiruvengadathan, A. Bezmelnitsyn, K. Gangopadhyay, S. Gangopadhyay
Department of Electrical and Computer Engineering
The University of Missouri
Columbia, MO, 65211

L. Polo-Parada
The Department of Medical Pharmacology and Physiology
The University of Missouri
Columbia, MO, 65211

ABSTRACT

This paper describes a new system for pressure-induced cell transfection. The system generates pressure pulses from a microchip that contains a small quantity of nanothermite material and an electrical igniter. The pressure output from the nanothermite reaction is coupled to the biological target through a PDMS membrane and a tube filled with gelatin. The system generates pressure pulses in the range of 10-40MPa. It has been used to transfect primary cells with 99% transfection rate and cell survival. It has also been used to transfect cell lines (Hela, HL-60, and HT-29). In all cases survival was >99%, and transfection rate in Hela, HL60 and HT-29 was up to 37 60 and 30% respectively. In addition, the system has been shown to transfect intact spinal cords and arteries from chicken (St 30) with no noticeable damage.

1. INTRODUCTION

One of the major obstacles in the development of gene therapy is the effective delivery of the genetic material into the target cells. (Orive et al. 2003) There are many existing techniques, which include physical, chemical, bacterial, and viral.(Baldi et al. 2007; Bergen et al. 2007; Cemazar et al. 2006; Chan et al. 2005; Gao et al. 2007; McCaffrey; Kay 2002; Plank et al. 2003; Racz; Hamar 2008; Recillas-Targa 2006; Rettig; Rice 2007; Simoes et al. 2005; White et al. 2007) However, what is lacking is a system that allows the maximal transfection rates (ideal >99%) with minimal damage (<1%) and high survivability rates (>99%).

One promising method is the use of pressure pulse to permeabilize cells. (Frairia et al. 2003; Kendall 2002; Kodama et al. 2000; Kodama et al. 2002, 2003; Koshiyama et al. 2006; Lee et al. 2000) The majority of research on shock-induced cell permeabilization has been conducted using energy sources based on either laser-ablation or gas-driven shock-tubes. Due to system limitations this research has resulted in low transfection rates of dyes.

An alternative approach to generating pressure waves, which has not been fully explored for drug delivery, is the energy profile generated by the reaction of energetic materials. This is mainly due to the narrow categories of conventional energetic materials (e.g. propellants or high explosives) and the limited ranges of performance tunability. The tunability of energetic output is essential to optimize delivery and minimize cell/tissue damage.

A relatively new finding is that certain types of nanothermite materials are capable of producing a unique pressure pulse when they are ignited.(Apperson et al. 2007) For example, the composition consisting of copper oxide (CuO) nanorods and aluminum (Al) nanoparticles has been shown to have combustion velocities in the same range as the heavy-metal azides, including metallic azides and fulminates but produce pressure levels much lower than those predicted by CJ theory.(Apperson et al. 2007; Bowden; Williams 1951; Shende et al. 2006a) In addition, these materials exhibit levels of performance tunability not seen within any conventional class of energetic materials.(Shende et al. 2006a; Shende et al. 2006b)

In this work, we present a micropyrotechnic-based system in which a nanothermite energy source is coupled to a biological target for gene transfer and drug delivery. Characterization of the pressure waves generated by the system is discussed, and the results of delivering plasmid into primary cells, cell lines, and tissues are presented.

2. EXPERIMENTAL

2.1 Nanothermite Preparation

Nanothermite mixtures consisting of Bi_2O_3 nanoparticles and Al nanoparticles were used for the transfection experiments reported herein. The Bi_2O_3

Report Documentation Page

Form Approved
OMB No. 0704-0188

1. REPORT DATE	2. REPORT TYPE	3. DATES COVERED
DEC 2008	**N/A**	**-**

4. TITLE AND SUBTITLE	5a. CONTRACT NUMBER
Nanothermite-Based Microsystem For Drug Delivery And Cell Transfection	5b. GRANT NUMBER
	5c. PROGRAM ELEMENT NUMBER
6. AUTHOR(S)	5d. PROJECT NUMBER
	5e. TASK NUMBER
	5f. WORK UNIT NUMBER
7. PERFORMING ORGANIZATION NAME(S) AND ADDRESS(ES) **Department of Electrical and Computer Engineering The University of Missouri Columbia, MO, 65211**	8. PERFORMING ORGANIZATION REPORT NUMBER
9. SPONSORING/MONITORING AGENCY NAME(S) AND ADDRESS(ES)	10. SPONSOR/MONITOR'S ACRONYM(S)
	11. SPONSOR/MONITOR'S REPORT NUMBER(S)

12. DISTRIBUTION/AVAILABILITY STATEMENT
Approved for public release, distribution unlimited

13. SUPPLEMENTARY NOTES
See also ADM002187. Proceedings of the Army Science Conference (26th) Held in Orlando, Florida on 1-4 December 2008, The original document contains color images.

14. ABSTRACT

15. SUBJECT TERMS

16. SECURITY CLASSIFICATION OF:			17. LIMITATION OF ABSTRACT	18. NUMBER OF PAGES	19a. NAME OF RESPONSIBLE PERSON
a. REPORT	b. ABSTRACT	c. THIS PAGE			
unclassified	**unclassified**	**unclassified**	**UU**	**8**	

nanoparticles were purchased from Accumet Materials Co., and they had particle sizes of 90-200nm. The Al nanoparticles were purchased from Novacentrix, and had average particle size of 80nm, with a 2.2nm oxide layer. The two types of particles were physically mixed in isopropanol (IPA) using ultrasonic agitation. Batches were mixed by dispersing 200mg of Bi_2O_3 in 1.5 mL of IPA by ultrasonic agitation for 30 minutes. Then 46.3mg of Al nanoparticles was added to the slurry and it was sonicated for an additional 4 hours. Then the mixture was dried in a convection oven at 90°C for 15minutes to remove all IPA. This powder was then loaded into the microchips.

2.2 Pressure Wave Generator Preparation

The pressure wave generator is shown in fig. 1. The system consists of a gel-filled tube, PDMS membrane, and a microchip that contains a small amount of nanothermite material and an integrated igniter. The nanothermite reaction produces a pressure wave, which propagates through the PDMS membrane and out of the end of the gel-filled tube. The PDMS membrane blocks the nanothermite material from traveling through the tube and coming in contact with the target of the pressure wave.

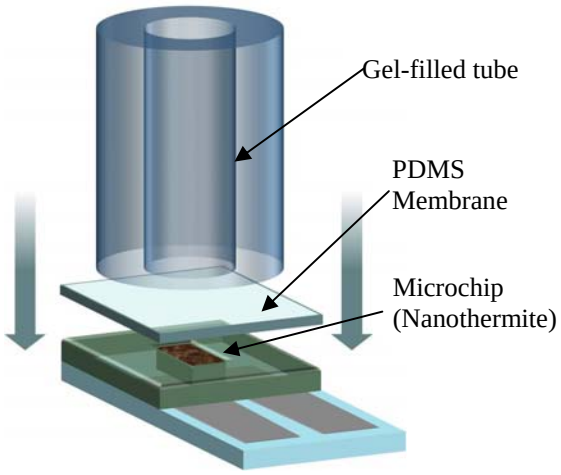

Fig. 1 Schematic of the system for generating pressure waves.

Typically each microchip consists of six or eight individual nanothermite pressure sources fabricated in a 25.4x25.4 mm square. The pressure sources were used individually; therefore, one microchip was used for multiple different particle delivery processes. A photograph of a microchip is shown in fig. 2.

The microchips were fabricated using two substrates. The microheaters were fabricated on a glass substrate using photoresist lift-off patterning, and sputter deposition of Pt/Ti thin-films. The wells were fabricated in a polycarbonate substrate by micro-drilling. The polycarbonate substrate was bonded to the glass substrate such that the wells were aligned over the microheaters. Bonding was carried out using a low-viscosity adhesive glue. Wires were bonded to the microheaters using soldering. Finally, the nanothermite material (in powder form) was loaded in the wells by manually packing.

Once the microchips were finished, a cured PDMS membrane (~1mm thick) was placed over the wells. The gel-filled transmission tube was made of stainless steel with a length of 25mm and internal diameter of 3.2mm. The gelatin used was from porcine skin and was dissolved in water (20% gelatin by weight). The gelatin was heated to 50°C, then injected into the steel tube and cooled to room temperature. A housing was used to hold the transmission tube onto the microchip and align the tube with each nanothermite energy source. The assembled device is shown in fig. 3. A standard 9V battery was used to power the microheaters and ignite the nanothermite material.

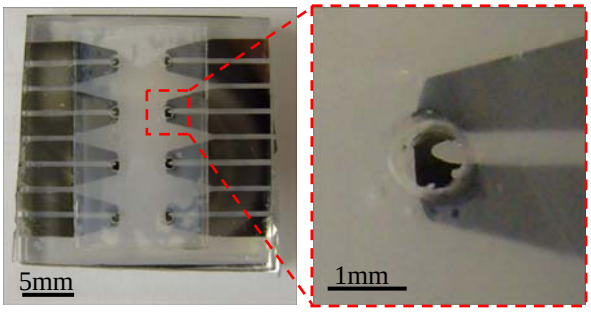

Fig. 2 Photograph of a microchip containing 8 individual sources.

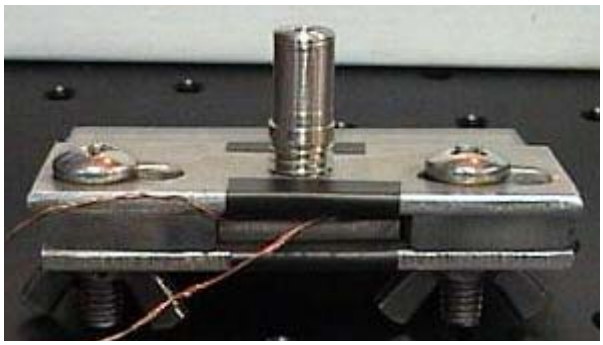

Fig. 3 Assembled pressure-wave generator.

2.3 Underwater Pressure Wave Characterization

The pressure wave generating characteristics of the nanothermite-based system have been experimentally investigated to understand how the system components affect the pressure impulse characteristics. The system used for characterizing the pressure waves is shown in supplemental figure 3. All tests were performed in water to simulate biological systems. All experimental conditions were tested 5 times to obtain averages and standard deviations.

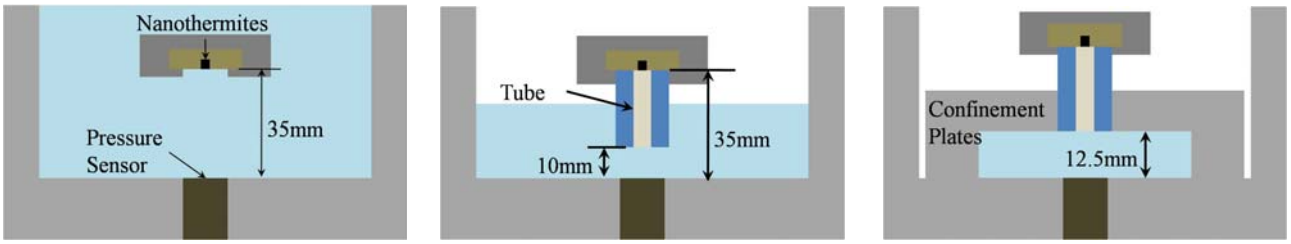

(A) (B) (C)

Fig.4 Characterization arrangements for measuring the pressure-generating characteristics of the system. (A) Configuration for measuring output directly from the microchip. (B) Configuration for comparing effect of PDMS and transmission tube. (C) Measurement configuration for closed target characterization.

A test bench was constructed for underwater testing of the pressure wave system. It consists of a small water vessel made from polycarbonate with internal dimensions of 4"x4"x3" (WxLxH), and wall thickness of 0.375". A pressure transducer (PCB 134A02) was mounted facing inward in the bottom of the vessel in the center. This transducer has a tourmaline sensing element (~3mm diameter), and it has a range of 137MPa, resonant frequency of 1.5MHz, and a rise time of 0.2µsec. The vessel was mounted to an optics breadboard. Stainless steel rods, fixed to the bench, were used to suspend the pressure wave generator in the tank, such that it was directed downward facing the pressure sensor. A high-speed camera (Photron Fastcam SA1.1) was used to record the interior of the tank, and it was used to correlate pressure transducer measurements to observable events. The micro-igniter in the pressure-wave generator was synchronized with the pressure sensor data acquisition and high-speed video recording by the same triggering switch.

The pressure generated directly from the microchip was investigated. The microchip was sealed with Parafilm, and completely submerged in the water vessel. This configuration is shown in fig. 4(A). Pressure-distance measurements were made by adjusting the height of the microchip above the pressure sensor. Microchips with different quantities of nanothermites were also tested.

The device was also prepared with the PDMS membrane and the gel-filled tube, and the output through the tube was measured. This configuration is shown in fig. 4(B). This configuration was compared with that shown in fig.4(A) to understand any changes in pressure-wave attenuation due to the PDMS membrane and gel-filled tube.

In addition, the vessel was configured to simulate *in vitro* test conditions. Specifically, plates were bolted to the bottom of the vessel to create the confined conditions that exist when cells or tissue samples are suspended with the genetic material for transfection experiments. The configuration of the vessel for these experiments is shown in fig. 4(C).

The confined volume that was created had cylindrical geometry. Different plates were used to create different internal volumes, and thus change the level of confinement. The height of the cylindrical volume was kept constant (12.5mm), but the diameter of the volume was changed (9mm to 53mm). This was used to investigate the confinement effect.

2.4 Cell/Tissue Transfection Experiments

The system used for transfection experiments is shown in Fig. 10. It was designed based on the results of pressure wave characterization. The target vessel was made from stainless steel and it had an internal cylindrical volume with 8mm diameter and 10mm height. A PCB 134A02 transducer was mounted in the bottom surface to monitor pressure inside the vessel during transfection.

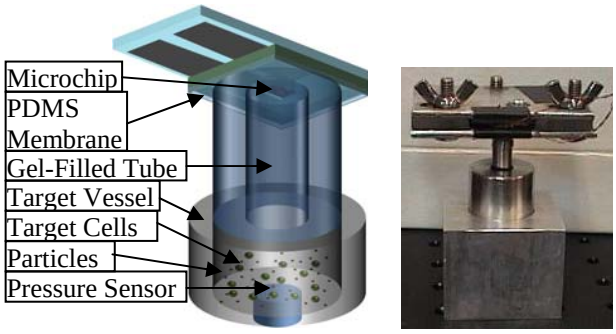

Fig. 10 Schematic (left) and photo (right) of the transfection testing system.

To test the effectiveness of our system for delivering materials into cells and tissues we used plasmid containing the information to express EGFP (enhanced green fluorescent protein) under the control of CMV (Human cytomegalovirus immediate early gene)

promoter. This plasmid, when properly inserted and expressed into cells, induces the production of EGFP inside the cells making them easily distinguishable by turning them fluorescent green.

We compared the transfection rates in primary cells (embryonic chicken heart cells) by our device with commercially available chemical methods (cationic lipid based reagents) and physical methods (electroporation). We also tested the efficiency of our system on cancer cell lines (adenocarcinoma epithelial cells (Hela), promyelocytic leukemia (HL60), and colonrectal adenocarcinoma (HT-29)), and tissues from the chicken embryo (spinal cord and artery).

Chick embryos were obtained from fertilized White Leghorn eggs (Hy-Line W-36, Hy-Line North America, LLC, West Des Moines, IA) and incubated for a 5d at 38^{o}C in an atmosphere of 80% humidity. The embryos (Stage 25) (according with HH(Hamburger; Hamilton 1951)) were removed from the egg and placed in a modified Tyrode solution of 140 mM NaCl, 5.6 mM KCl, 1.85 mM $CaCl_2$, 0.5 mM $MgCl_2$, 10 mM $NaHCO_3$, 1.8 mM NaH_2PO_4, 5.5 mM Glucose, at 37^{o}C and gassed with a mixture of 95% O2 and 5% CO_2, with a pH of 7.3-7.4. The hearts were then separated from the embryo and processed for single cell dissociation.

The cells were dissociated from the atrium or ventricle with Papain (Worthington, Lakewood, NJ) according to the manufacturer's protocol. Briefly, Papain was activated for 30 min at 37 ^{o}C by the addition of β-mercaepthanol, ethylendiaminetetraacetic acid (EDTA) and L-cystein. Atrial and ventricular tissues were incubated in a Papain solution in a Hanks Balanced Salt (HBBS) solution of Ca^{2+} and Mg^{2+} free for 5 to10 minutes. Then the Papain was inactivated by the addition of a cold HBBS containing 1mg/ml trypsin inhibitor soybean, followed by washing the tissue/cells twice with a cell culture medium. Cells were dissociated by pipetting the tissue 5 to 10 times through a small diameter end-fire-polished glass Pasteur pipette. If the tissue was dissociated into single cells before the washing step, the cells were pelleted by centrifugation at 800 g for 3 to 5 minutes.

The spinal cord and artery (ventral laminectomy) were isolated from an embryo St 30. The spinal cord was chosen because of its fragile nature in order to test whether the pressure waves produce any damage to the tissue. The arteries were selected because they are tough tissue (due to the large amounts of extracellular matrix and connective tissue present in these tissues), which is difficult to transfect.

The cell lines Hela, HL-60, and HT-29 were obtained from ATCC (Manassas, VA), and propagated and cultured as recommended by the ATCC. For each test the adherent cells were resuspended in 10 ml TrypLE Express (Gibco, Invitrogen) for 10 min. Then, they were pelleted by centrifugation at 800g for 5 min and washed 3 times and resuspended with the media recommended by ATCC. An average of 10 E^3 cells/test were used. A sample of each batch of cells was used to evaluate cell condition, using a Trypan Blue staining and a hematocytometer to quantify the number of viable vs. death cells.

2.5 Transfection Procedure

The cells/tissues were transfected with 0.5 μg of plasmid/test. After the procedure the cells/tissue were transferred into 35 mm culture dishes with an insert of a circular 25 mm glass cover slip (Fisher Scientific). For the cell cultures, the cells were seeded in the glass cover slip for 1-2 hr into the incubator to allow the cells to attach to the substrate. Then cell culture dish was carefully filled with 2 ml of fresh culture media and kept it in the incubator with an atmosphere of 10% CO_2 for 24 hrs.

Cardiomyocytes obtained with this method were attached to the dish bottom and exhibited spontaneous contractions after 2 to 3 hours in culture. Single isolated cells were cultured with a Neurobasal medium supplemented with B-27, Glutamax, insulin-transferrin-selenium-A, penicillin and streptomycin (Invitrogen).

2.6 Survival Analysis

To evaluate the number of dead or dying cells in all the cells and tissues, we used the vital dye - Trypan Blue, Orange Nucleic Acid Stain (SYTOX), Hoechst 33258, and YO-PRO-1. Trypan blue chromopore is negatively charged and does not interact with the cell unless the membrane is damaged; therefore, all the cells which exclude the dye are viable. SYTOX is a high affinity nucleic acid stain that easily penetrates cells with compromised plasma membranes. Hoechst stains the condensed chromatin of apoptotic cells brighter than the chromatin of normal cells. YO-PRO-1 passes through the plasma membrane of both apoptotic and necrotic cells.

In order to evaluate cell viability, we used the cell-permeant dye calcein AM. In living cells the non-fluorescent dye is converted to a green-fluorescent calcein, after acetoxymethyl ester hydrolysis by intracellular esterases. To evaluate the general health of our transfected cells we detected proliferating cells in our cultures using EdU (5-ethynyl-2´-deoxyuridine, which is a nucleoside analog containing an alkyne) cell proliferation assay (Click-iT, Invitrogen).

2.7 Optical Imaging and Transfection Rate Analysis

After 24 hrs of incubation of the cells/tissues, the samples were fixed by replacing the culture media with a solution containing 70% ETOH for at least 4 hrs at 4°C. Samples were rinsed 5x 5min with PBS and kept in PBS solution at 4°C until the cells/tissues were analyzed. Following rinsing, cells were visualized with a 40x water immersion objective on an Olympus microscope equipped with the appropriate filter cubes (FITC-Semrock-zero pixel shift, Rochester, NY). Images were digitally captured with an upright BX51 WI Olympus (Olympus America Inc. Center Valley, PA) microscope equipped with a Retiga EXi Fast1394 (Qimaging, Surrey, BC Canada) digital camera or Axiocam mRC (Zeiss, Jena, Germany). The images were processed with Qcapture Pro, Adobe Photoshop or Corel Draw. The montage and labeling of the colored images were created using Corel Draw 12. To determine the degree of transfection, the mean pixel intensity of a ROI (Region of Interest) for each cell was measured using QCapture Pro (Qimaging Inc). Only cells that exhibited at least 4x the mean autofluoresence measured in control cells were consider in this study. At least 100 single isolated cells/dish/conditions were evaluated. For quantification, we used the same exposure time for all the pictures (600 msec-Retiga camera). For presentation, we used the Axiocam camera with an exposure of 1.3 sec for all the pictures.

3. RESULTS AND DISCUSSION

3.1 Pressure-Wave Characterization

Figure 5 shows pressure-distance data for nanothermites. The nanothermites were tested in the configuration shown in fig. 4(A). The nanothermites tested in this series were 3mg of Bi_2O_3/Al (red plot), and 1.4mg of CuO/Al (black plot). The overpressure of the nanothermite pressure waves is significantly lower than silver azide.(Saito et al. 2003)

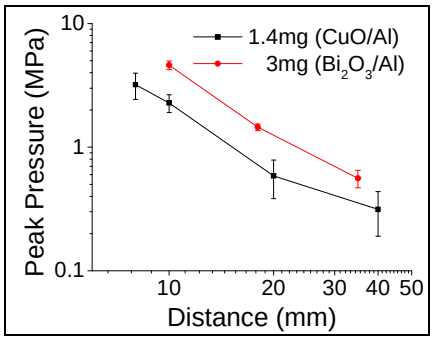

Fig. 5 Peak pressure vs. distance for nanothermites in microchips.

Fig. 6 shows a comparison of pressure profiles measured in the configurations if Fig. 4(A) and Fig. 4(B). These profiles are for microchips containing 3mg of Bi_2O_3/Al. The distance between the nanothermite source and the pressure sensor was the same in both conditions. The only difference is the presence of the coupling elements (PDMS membrane and gel-filled tube). It appears from the comparison of these profiles that the shock wave which leads the blast wave is transmitted through the tube, with perhaps less attenuation than when the tube and PDMS is not present. It also appears that the coupling elements block most of the expansion wave that follows behind the shock front. This is due to the blocking of the reaction products (solid and gaseous) by the PDMS membrane.

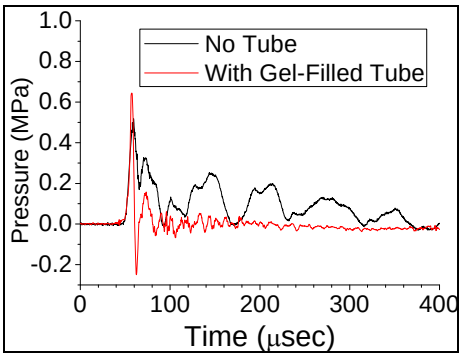

Fig. 6 Comparison of pressure profiles with and without the PDMS membrane and gel-filled tube.

The plot in Fig. 7 is the profiles for varying the diameter of the confinement volume and the open system. These tests were all performed using microchips containing 3mg of Bi_2O_3/Al. All the profiles contain the high-frequency shock wave component that is observed in open systems. However, when the confinement volume is small, there is another component of the pressure pulse is observed. When the diameter of the confinement volume goes below ~20mm, the broad pulse is the dominant energy that is seen by the sensor.

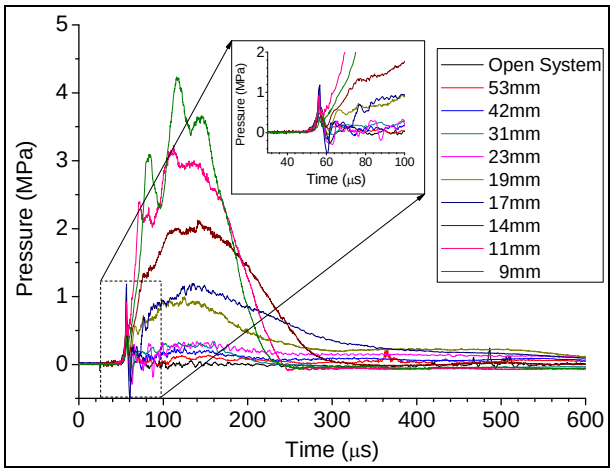

Fig. 7 Pressure-time histories for experiments varying the diameter of the confinement volume. The plot legend lists the diameter of the internal volume.

Fig. 8 is a plot of the pulse characteristics as diameter of the volume changes. The shock wave intensity and broad pulse intensity are expressed in MPa and the total impulse is expressed in Pa-s. The total impulse was obtained by numeric integration of the entire pulse.

There does not appear to be any correlation between the intensity of the shock pulse and the dish diameter, but the intensity of the broad pulse gets larger as the dish size decreases. The total impulse varies consistently with the size of the confinement volume, increasing as the internal volume decreases.

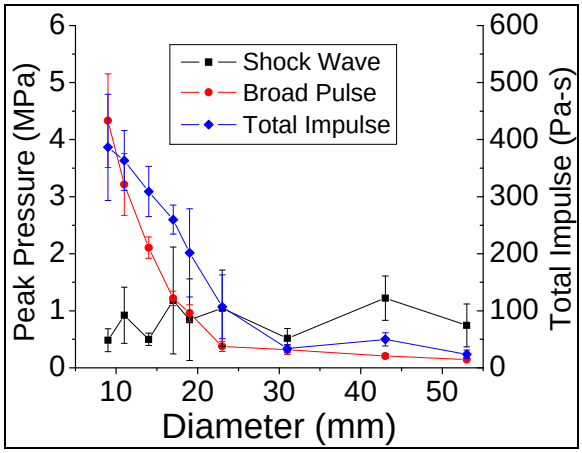

Fig. 8 Shock wave intensity, broad pulse intensity, and total impulse vs. vessel diameter.

Analysis of the high speed video gave insight into the reason for the observation of large pressure pulses in the smaller dishes. As shown in Fig. 9, some of the gelatin in the tube protrudes out of the end and into the target dish. It is believed that as the size of the dish decreases, the gelatin begins to behave like a piston, elevating the pressure inside the vessel, and causing the broad pressure pulse seen in the profiles for small vessels. Assuming that the gelatin is having a piston effect in the system, then it would be a sub-sonic event, and the pressure it generates would be uniform throughout the vessel.

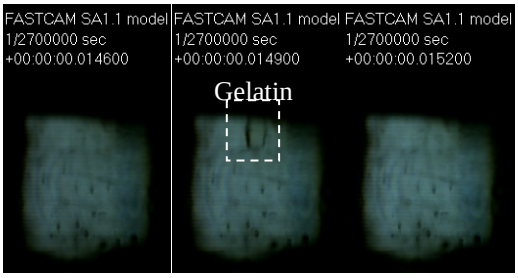

Fig.9 High-speed video images of gel protruding from the end of the tube into the target vessel.

3.2 Cell Transfection Experiments

Fig. 10 shows transfection rate and survival of chicken primary cells using various methods. Primary cells, in particular cardiomyocyte are well known to be difficult to transfect with diverse non-viral methods/materials (Djurovic et al. 2004; Kott et al. 1998; Muramatsu et al. 1997). In general transfection of chick cardiomyocyte with different non-viral commercially available transfection methods induces limited transfection efficiency with very large mortality (Djurovic et al. 2004; Kott et al. 1998; Muramatsu et al. 1997). However our device induces very large transfection and survivability rates. Fig. 11 shows microscope images of the cells transfected with the nanothermite system.

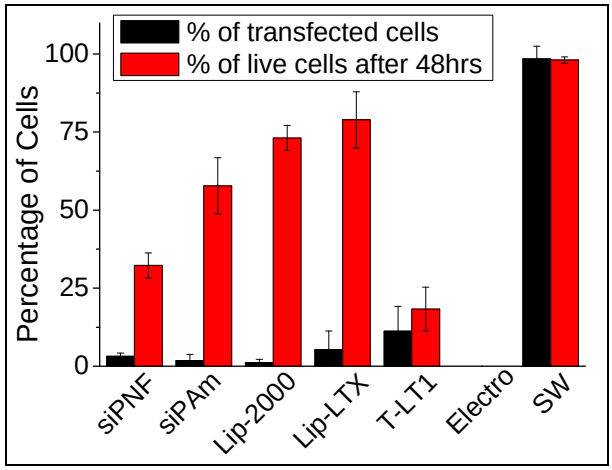

Fig. 10 Transfection and survival rates of chicken primary cells by different methods. (Electro = electroporation, SW = Nanothermite system)

Fig. 11 Microscope images of chicken primary cells transfected using nanothermite system. (Left) Transmission-mode image. (Right) Fluorescence image.

Testing of the different cells lines produced a more modest transfection rate; however, cell survivability was similar in all the tested cells (> 99%). Furthermore, we were able to enhance transfection rates in cell lines without reducing survivability by increasing the pressure wave amplitude and total impulse [14, 19]. This was achieved by fabricating microchips in which each pressure wave source contained a larger quantity of nanothermites (increased from 3mg to 15mg). The configuration change resulted in the increase of the pressure wave amplitude and total impulse from 12.0±2.3 MPa to 20.1±3.5 MPa and from 483±67 Pa-s to

1,289±130 Pa-s respectively. Fig. 12 shows transfection rate in each cell line using the two different size pulses. Fig. 13 shows microscope images of the cells transfected using the larger pulse.

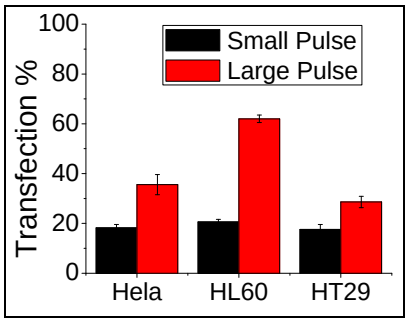

Fig. 12 Transfection rate of cancer cell lines using different strengths of pulse generating microchips.

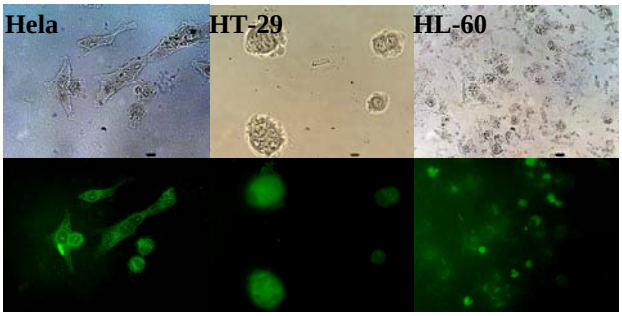

Fig. 13 Microscope images of cancer cells transfected using nanothermite system. (Top) Transmission-mode imaging. (Bottom) Fluorescence-mode imaging.

In the tissues (spinal cord and artery), significant levels of GFP expression in all tissues, and no significant damage was observed. However, transfection and survival rate was not quantified due to difficulty of counting individual cells inside the tissues. Fig. 14 shows fluorescence microscope images of the tissues (spinal cord and artery) from the chicken.

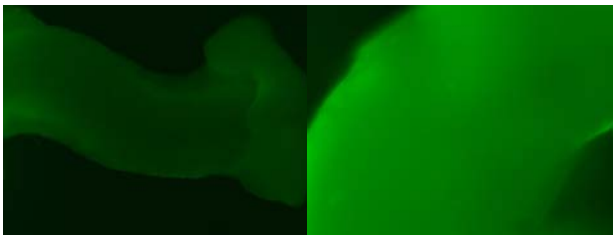

Fig. 14 Fluorescence microscope images of transfected Spinal cord (Left) and artery (Right).

CONCLUSION

A new system has been developed for *in vitro* transfection of cells and tissues. The system utilizes a microchip-based pressure generator based on nanothermite reactions. The system operates based on generation of shock waves and subsonic compression of the target biological medium to permeabilize cells. Further studies are required to investigate whether or not one of these pressure-generating mechanisms is responsible for cell permeabilization. Never the less, this system has been shown to deliver plasmid, and induce expression of GFP. Successful transfection was demonstrated in primary cells, cell lines, and tissues. The use of microchip technology maintains the potential for system integration with other *in vitro* lab-on-chip systems, as wells as the potential for compact *in vivo* gene transfer devices.

REFERENCES

Apperson, S., and Coauthors, 2007: Generation of fast propagating combustion and shock waves with copper oxide/aluminum nanothermite composties. *Applyed Physics Letters*, **1**.

Baldi, L., D. L. Hacker, M. Adam, and F. M. Wurm, 2007: Recombinant protein production by large-scale transient gene expression in mammalian cells: state of the art and future perspectives. *Biotechnol Lett*, **29,** 677-684.

Bergen, J. M., I. K. Park, P. J. Horner, and S. H. Pun, 2007: Nonviral Approaches for Neuronal Delivery of Nucleic Acids. *Pharm Res*.

Bowden, F. P., and H. T. Williams, 1951: Initiation and Propagation of Explosion in Azides and Fulminates. *Proc. R. Soc. London*, **208,** 176-188.

Cemazar, M., M. Golzio, G. Sersa, M. P. Rols, and J. Teissie, 2006: Electrically-assisted nucleic acids delivery to tissues in vivo: where do we stand? *Curr Pharm Des*, **12,** 3817-3825.

Chan, S. A., L. Polo-Parada, L. T. Landmesser, and C. Smith, 2005: Adrenal chromaffin cells exhibit impaired granule trafficking in NCAM knockout mice. *J Neurophysiol*, **94,** 1037-1047.

Djurovic, S., N. Iversen, S. Jeansson, F. Hoover, and G. Christensen, 2004: Comparison of nonviral transfection and adeno-associated viral transduction on cardiomyocytes. *Mol Biotechnol*, **28,** 21-32.

Frairia, R., M. G. Catalano, N. Fortunati, A. Fazzari, M. Raineri, and L. Berta, 2003: High energy shock waves (HESW) enhance paclitaxel cytotoxicity in MCF-7 cells. *Breast Cancer Res Treat*, **81,** 11-19.

Gao, X., K. S. Kim, and D. Liu, 2007: Nonviral gene delivery: what we know and what is next. *Aaps J*, **9,** E92-104.

Hamburger, V., and H. L. Hamilton, 1951: A series of normal stages in the development of the chick embryo. *J. Morph*, **88,** 49-92.

Kendall, M., 2002: The delivery of particulate vaccines and drugs to human skin with a practical, hand-held shock tube-based system. *Shock Waves*, **12,** 23-30.

Kodama, T., M. R. Hamblin, and A. G. Doukas, 2000: Cytoplasmic molecular delivery with shock waves: importance of impulse. *Biophys J*, **79,** 1821-1832.

Kodama, T., A. G. Doukas, and M. R. Hamblin, 2002: Shock wave-mediated molecular delivery into cells. *Biochim Biophys Acta*, **1542,** 186-194.

——, 2003: Delivery of ribosome-inactivating protein toxin into cancer cells with shock waves. *Cancer Letters*, **189,** 69-75.

Koshiyama, K., T. Kodama, T. Yano, and S. Fujikawa, 2006: Structural change in lipid bilayers and water penetration induced by shock waves: molecular dynamics simulations. *Biophys J*, **91,** 2198-2205.

Kott, M., A. Haberland, S. Zaitsev, B. Buchberger, I. Morano, and M. Bottger, 1998: A new efficient method for transfection of neonatal cardiomyocytes using histone H1 in combination with DOSPER liposomal transfection reagent. *Somat Cell Mol Genet*, **24,** 257-261.

Lee, S., D. McAuliffe, T. Kodama, and A. Doukas, 2000: In Vivo transdermal delivery using a shock tube. *Shock Waves*, **10,** 307-311.

McCaffrey, A. P., and M. A. Kay, 2002: A story of mice and men. *Gene Ther*, **9,** 1563.

Muramatsu, T., Y. Mizutani, Y. Ohmori, and J. Okumura, 1997: Comparison of three nonviral transfection methods for foreign gene expression in early chicken embryos in ovo. *Biochem Biophys Res Commun*, **230,** 376-380.

Orive, G., R. M. Hernandez, A. R. Gascon, A. Domınguez-Gily, and J. L. Pedraz, 2003: Drug delivery in biotechnology: present and future. *Current Opinion in Biotechnology*, **14,** 659-664.

Plank, C., and Coauthors, 2003: The magnetofection method: using magnetic force to enhance gene delivery. *Biol. Chem*, **384,** 737-747.

Racz, Z., and P. Hamar, 2008: [SiRNA technology, the gene therapy of the future?]. *Orv Hetil*, **149,** 153-159.

Recillas-Targa, F., 2006: Multiple strategies for gene transfer, expression, knockdown, and chromatin influence in mammalian cell lines and transgenic animals. *Mol Biotechnol*, **34,** 337-354.

Rettig, G. R., and K. G. Rice, 2007: Non-viral gene delivery: from the needle to the nucleus. *Expert Opin Biol Ther*, **7,** 799-808.

Saito, T., M. Marumoto, H. Yamashita, S. H. R. Hosseini, A. Nakagawa, T. Hirano, and K. Takayama, 2003: Experimental and numerical studies of underwater shock wave attenuation. *Shock Waves*, **13,** 139-148.

Shende, R., and Coauthors, 2006a: Nanostructured Energetic Materials, Session M,. *25th Army Science Conference, Orlando, Fl.*

——, 2006b: Nanoenergetic Composites of CuO Nanorods, Nanowires, and Al-Nanoparticles. *Propellants, Explosives, Pyrotechnics*.

Simoes, S., A. Filipe, H. Faneca, M. Mano, N. Penacho, N. Duzgunes, and M. P. de Lima, 2005: Cationic liposomes for gene delivery. *Expert Opin Drug Deliv*, **2,** 237-254.

White, K., S. A. Nicklin, and A. H. Baker, 2007: Novel vectors for in vivo gene delivery to vascular tissue. *Expert Opin Biol Ther*, **7,** 809-821.